ASTRONOMY & ASTROPHYSICS
SUPPLEMENT SERIES

Astron. Astrophys. Suppl. Ser. **101**, 37-47 (1993)

Anomalous proper motions in the Cygnus Superbubble region

F. Comerón[1], J. Torra[1], C. Jordi[1] and A.E. Gómez[2]

[1] Departament d'Astronomia i Meteorologia, Universitat de Barcelona, Av. Diagonal, 647, E-08028 Barcelona, Spain
[2] Département d'Astrophysique Stellaire et Galactique, Observatoire de Paris, Meudon, Place Jules Janssen, 8, F-92195 Meudon, France

Received August 5, 1992; accepted January 18, 1993

Abstract. — In an analysis of proper motions of O and B stars contained in the Input Catalogue for Hipparcos, we have found a clear deviation from the expected pattern of systematic motions which can be readily identified with the associations Cygnus OB1 and Cygnus OB9, located near the edge of the Cygnus Superbubble. The anomalous motions are directed outwards from the center of the Superbubble, which is coincident with the association Cygnus OB2. This seems to support the hypothesis of a strong stellar and supernova activity in Cygnus OB2 giving rise to the Superbubble and, by means of gravitational instabilities in its boundaries, to Cygnus OB1 and Cygnus OB9. New $uvby\beta$ aperture photometry of selected O and B stars in the area of Cygnus OB1 and Cygnus OB9 is also presented and analyzed in this paper.

Key words: stars: early type — interstellar medium: bubbles — open clusters and associations: Cygnus OB1, Cygnus OB9

1. Introduction

The region lying in the plane of the Milky Way in the direction of the constellation Cygnus displays one of the richest accumulations in the sky of objects related to recent and current star forming activity. The line of sight runs roughly parallel to the path of the Orion-Cygnus spiral arm (Elmegreen 1985) between galactic longitudes $70^o < l < 90^o$, and the bright spiral arm tracers spread along the arm are thus observed from our vantage point as a concentration of objects with different heliocentric distances covering a comparatively small area in the sky.

A significant part of this area, below galactic longitude $l < 85^o$, is occupied by the Cygnus X region, a multiple extended radio source which has been studied in many frequencies (see e.g. Piepenbrink & Wendker 1988, and references therein). Other large scale objects in the region include OB associations and open clusters (Ruprecht 1966; Humphreys 1978; Lyngå 1987), HII regions (Blitz et al. 1982; Piepenbrink & Wendker 1988; Lockman 1989), HI supershells (Heiles 1979, 1984) and a possible extended X ray source known as the Cygnus Superbubble (Cash et al. 1980). An extensive account of the observational material available on that region has been published by Bochkarev & Sitnik (1985).

In this paper, we present results on the analysis of proper motions available for some early type stars of the Cygnus region, revealing an anomalous behaviour which may give some valuable clues on the nature of the Cygnus Superbubble. Also presented are new photometric observations in the Strömgren system of selected O and B stars presumably belonging to the associations Cygnus OB1 and Cygnus OB9.

In Sect. 2, we give an overview on published observations of the Cygnus Superbubble and their interpretations. Section 3 deals with the OB associations lying in the area, paying particular attention to the problems found when trying to determine their distances to the Sun. In Sect. 4 we discuss the evidence for anomalous proper motions of the stars belonging to some of the associations. Section 5 describes the new photometric observations carried out by us. The main conclusions are summarized in Sect. 6. Theoretical analysis of the consequences of the results reported here is deferred to a further paper.

2. The Cygnus Superbubble

The discovery of an extended X-ray ring-like source by Cash et al. (1980) was interpreted as an evidence for the existence of a large structure sharing a physical relationship with previously known optical and radio sources in the neighbouring region. The estimated thermal energy of the bubble, its spatial coincidence with the HI shell GS081-05-37 and the proximity of the association Cygnus OB2 to its center seem indeed to support the view of a single structure owing its origin to the energetic processes taking place in very massive stars at the early evolutionary stages of OB associations like Cygnus OB2. At the distance of Cygnus OB2 adopted by Cash et al., the Superbubble should have a diameter of 450 pc, and the observed X-ray output would imply a thermal energy of 6 10^{51} erg at a temperature of 2 10^{6} K. This diameter would make the Cygnus Superbubble one of the largest supershells of the Galaxy. The energetic content can only be explained by assuming a chain of highly synchronous energetic events in Cygnus OB2, in the form of strong stellar winds and supernova explosions.

This interpretation has been called into question more recently. Bochkarev & Sitnik (1985) showed that the X-ray luminosity of the Superbubble may be accounted for by considering the contributions of known individual compact X-ray sources and the hot coronae around OB associations. Moreover, the Cygnus X radio source, which Cash et al. (1980) proposed to be related to the Superbubble, is likely to consist of an arrangement of unrelated objects along the line of sight, as suggested by Dickel & Wendker (1978), Wendker (1984) and Piepenbrink & Wendker (1988).

The single-structure interpretation and the line-of-sight arrangement interpretation are not necessarily incompatible with each other, since, given the location of this region in the Orion-Cygnus spiral arm, a high degree of foreground and background contamination from unrelated sources is to be expected on any extended area; the question then focuses on whether this contamination can account for its entire appearance. A crucial point in deciding the physical entity of the observed arrangement of sources is the ability of plotting a three dimensional map where a distance to the Sun is assigned to each object. Kinematic distances are only very poor distance indicators in this region, because galactic differential rotation introduces only a small systematic effect on the observed radial velocities up to a distance of 3-4 kpc, and the distances to most of the sources are thus very uncertain unless they are clearly associated with stellar objects for which spectrophotometric distances can be calculated.

3. OB associations in Cygnus

The IAU catalog of OB associations (Ruprecht 1966) lists seven objects in Cygnus and two more doubtful candidates. O and B type stars and supergiants belonging to these associations have been listed by Humphreys (1978) and Humphreys & McElroy (1984). These works contain compilations of *UBV* photometric data from different sources, and programs are in progress to obtain more homogeneous databases for stars in the associations (Garmany & Vacca 1991; Garmany & Stencel 1992). In practice, the individual stellar distances show a large spread, and the resulting uncertainty in the average distance of the association is considerable. Another source of error is the inclusion of non-members in the average, which may systematically bias the results. This problem is especially troublesome in a crowded area like Cygnus. As a consequence, the distances to Cygnus OB associations are determined with uncertainties of several hundred parsecs, which are of the same order as the distances among them. As some of these associations overlap when projected on the celestial sphere, the possibility that some of them that are catalogued as separate objects may be parts of a single group cannot be ruled out. In Table 1, we have listed the limits in galactic longitude l and latitude b of the OB associations in Cygnus as given in existing works. We also list the range of distances determined in different studies for each association, as compiled by Humphreys (1978). The large spread for some of them is evident and reflects the difficulty in obtaining reliable distances.

Table 1. Published parameters of OB associations in Cygnus

Name	l	b	d (pc)	notes
Cygnus OB1	74°/77°	−0°6/2°8	1250 – 1830	
Cygnus OB2	80°1	0°9	1440 – 2100	
Cygnus OB3	71°3/73°8	1°2/3°4	1580 – 2510	
Cygnus OB4	81°/84°	−8°3/−6°3	1000	
Cygnus OB5	64°2/70°0	−2°7/6°9	1610	doubtful
Cygnus OB6	83°/89°	−3°/5°	1700	doubtful
Cygnus OB7	84°/96°	−4°9/9°0	740 – 800	
Cygnus OB8	76°3/79°2	2°1/5°4	2190 – 2320	
Cygnus OB9	77°/79°	0°8/2°2	1170 – 1200	

A somewhat more reliable method for determining distances to OB associations is by main sequence fitting of open clusters physically related to them. There are 9 open clusters in the catalog of Lyngå (1987) lying in the western region of the Superbubble, where most of the OB associations are located. Their characteristics are listed in Table 2. The quoted distances and ages are those derived by Janes et al. (1988) from a weighted average of different determinations, when available.

Table 2. Open clusters near Cygnus OB1, OB3, OB8, OB9

Name	l	b	d (pc)	age (10^6 yr)
NGC 6871	72°6	2°1	1750	12
Biurakan 2	72°8	1°3	1500	10
NGC 6883	73°3	1°2	1380	15
Basel 6	74°9	3°3	2100	
IC 4996	75°4	1°3	1560	10
Berkeley 87	75°7	0°3	840	10
Berkeley 86	76°7	1°3	1110	40
NGC 6913	76°9	0°6	1340	10
NGC 6910	78°7	2°0	1510	

It is difficult to interpret these data in view of the large distance uncertainties and to decide what associations and clusters are in fact parts of single complexes, particularly for the overlapping regions Cygnus OB1, OB3 and OB9. From the shortest distance estimates and the distances of likely associated clusters (NGC 6913 and IC 4996 to Cygnus OB1, NGC 6871 to Cygnus OB3 and NGC 6910 to Cygnus OB9), it seems possible that Cygnus OB1 and Cygnus OB9 really constitute a single stellar complex, with Cygnus OB3 being in the background. Cluster Basel 6, with a distance much larger than those of the other clusters, does not seem to be related to any OB association. Berkeley 86 and Berkeley 87 are seen in the direction of Cygnus OB1, but the distance of Berkeley 87 is shorter than those deduced both from the stars presumably belonging to the association and the possibly related clusters, and may be a foreground object. Berkeley 86, on the other hand, has no stars earlier than B3, thus indicating an age of 40 10^6 yr, which is longer than the lifetime of an OB association before dispersing into the surrounding medium, and is probably a foreground unrelated object.

This same distance uncertainty appears in Cygnus OB2, a very compact association containing some of the brightest early-type stars detected in our Galaxy (Humphreys 1978; Hutchings 1981; Leitherer et al. 1982; Torres-Dodgen 1990). The difficulty in determining the distance to Cygnus OB2 is enhanced both by the peculiarities of its brightest members and by the strong foreground extinction of $A_V \simeq 5$ mag. These problems have been stressed by Torres-Dodgen et al. (1991), who obtained the most accurate distance determination to date as $d = 1700 \pm 200$ pc.

Interstellar extinction in the direction of Cygnus shows a remarkable degree of patchiness (Lucke 1978; Dickel & Wendker 1978). A large portion of the area of our interest lies behind the Great Rift dividing the Milky Way into two branches at Cygnus. Dickel & Wendker (1978) have found $A_V \simeq 4-5$ mag in the Cygnus X region, and less than 2 mag west of it in the area occupied by Cygnus OB1, OB3, OB8 and OB9.

Evidences of the strong interaction between stars in Cygnus OB1 and the interstellar medium surrounding the association have been observed as a hierarchical systems of shells (Lozinskaya & Sitnik 1988; Lozinskaya & Repin 1990), and high velocity gas associated to the shells is observed superimposed on the UV spectra of association stars (St. Louis & Smith, 1991).

4. Evidence for anomalous proper motions

The stellar sample we have used to analyze the stellar motions in Cygnus is composed of 14,147 O and B stars belonging to the Proposal 99 for Hipparcos (Turon et al. 1992). These data are retrieved from the Input Catalogue (INCA) database (Gómez et al. 1989b). The spectral types in the Cygnus region are mostly coming from the SIMBAD database. Positions and proper motions are from the CDA (Catalogue de Données Astrometriques) compilation of astrometric data (Jahreiβ 1989) included in the INCA database. All these data have been transferred to the FK5 system (Fricke et al. 1988) for epoch 1990.0 and equinox J2000.0. The CDA astrometric data in the Cygnus region were almost entirely taken from the PPM compilation (Röser & Bastian 1991). The estimated mean error for each component of the proper motion as quoted in the PPM is 0"004 yr^{-1}.

The completeness of the INCA database has been discussed elsewhere (Gómez et al. 1989a). Limiting magnitude for 100 % completeness varies between $V = 7.3$ for $b = 0^o$ and $V = 8.3$ for $|b| > 20°$. However, although with a decreasing degree of completeness, many fainter stars in the region of Cygnus have been included in INCA.

Figure 1 shows a plot of 380 O and B stars from the IC 99 catalog in the Cygnus region. Most of stars lie in the area occupied by Cygnus OB1, OB2, OB3 and OB9. The association Cygnus OB8 also lies in the same area; however, it is too distant for most of its stars to appear in our catalog. Likely foreground stars have been partially eliminated by calculating a spectrophotometric distance according to the method described by Arenou et al. (1992) and removing those located at less than 500 pc from the Sun.

The galactic longitude vs. proper motion in longitude of 278 O and B stars having known proper motions shown in Fig. 2 clearly shows a systematic deviation from the expected pattern of proper motions from the galactic rotation. The dashed line in Fig. 2 represents the systematic proper motions for stars located at a distance of 1400 pc from the Sun expected from a pure axisymmetric pattern of differential galactic rotation. We have used parameters for a flat rotation curve ($A = -B = 13$ km $\mathrm{s}^{-1}\mathrm{kpc}^{-1}$; Kerr & Lynden-Bell 1986), and the standard value of the solar motion, $U_\odot = 10.0$ km s^{-1}, $V_\odot = 15.4$ km s^{-1}, $W_\odot = 7.8$ km s^{-1}. Reasonable changes on all of these quantities or on the assumed distance introduce only a small modification in Fig. 2 and do not alter the conclusion that most of the stars in the interval $72° < l < 79^o$ fall below the expected systematic motion. No such appreciable anomaly is detected in the proper motions in galactic latitude. Although it is possible that some of these stars do not lie at the assumed distance of 1400 pc, we do expect that most of them belong to associations, given the distinct appearance of these in Fig. 1.

Further evidence for the anomalous proper motions of these stars comes from Fig. 3, where the spectrophotometric parallaxes of the stars in Fig. 2 are plotted against the proper motions in longitude. Although large scatter exists on the horizontal axis due to the uncertainties in the derived parallax, a significant trend towards grouping below the expected systematic motion is clear. The dashed

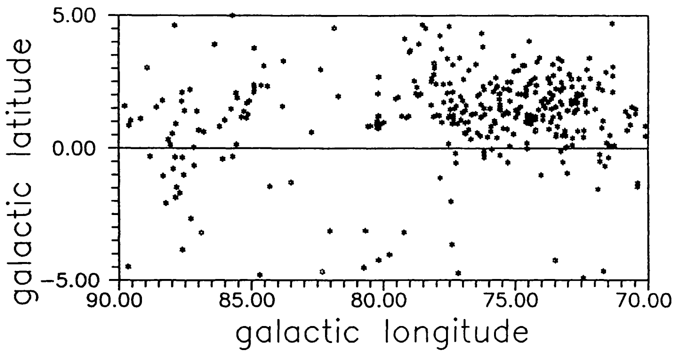

Fig. 1. O and B stars included in IC 99 in the Cygnus region with $d > 500$ pc

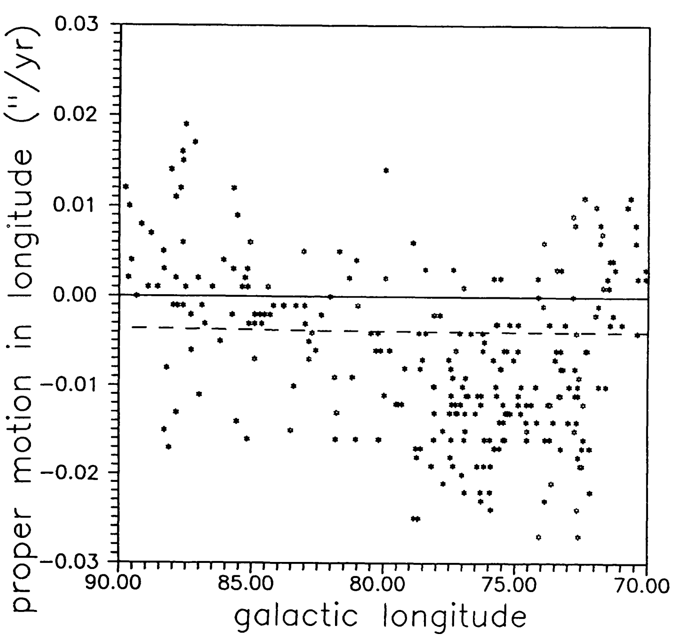

Fig. 2. Galactic longitude and proper motion of the stars plotted in Fig. 1 having known proper motions. It is evident a clustering of stars below the dashed line which represents the expected systematic proper motions of stars at a distance of 1400 pc

line now corresponds to the expected proper motions of stars at $l = 75^o$. The concentration of anomalous proper motions is stronger at π" $\simeq$ 0"0006, in a rough agreement with the distances to Cygnus OB1 and OB9 discussed in the preceding section.

4.1. Are the proper motions real?

The possibility that the anomalous proper motions reflect a systematic error in the astrometric data instead of a real effect cannot be discarded beforehand. Although the systematic residuals between the FK5 and the PPM systems are in general well below the value of the anomaly detected by us (Röser & Bastian 1991), this might not hold for the very early-type stars we are interested in, which are known to be difficult astrometric objects. We have thus conducted a series of statistical tests to check for the signification of the anomalous motions and to rule out the possibility of a number of systematic effects which might make it appear the anomaly as it is observed.

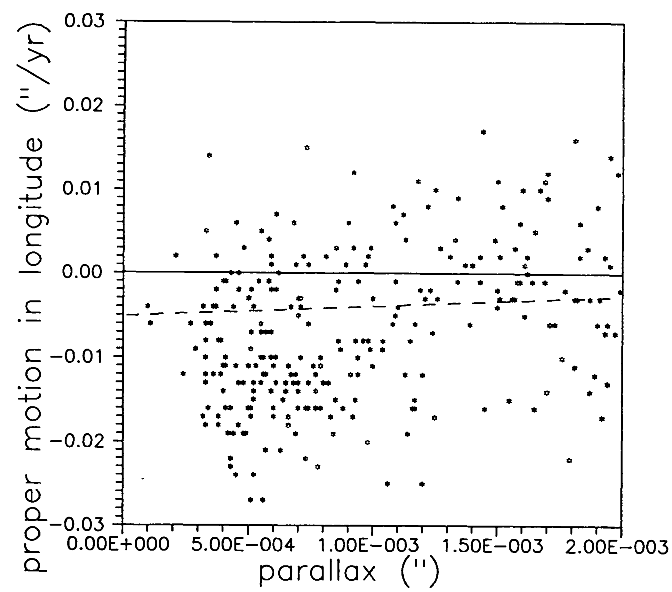

Fig. 3. Parallax and proper motions of the stars plotted in Fig. 2. The stars with anomalous proper motions appear as a distinct clump below the dashed line (which represents the expected systematic motions at their mean galactic longitude) at a mean parallax π" = 0"0008. Parallaxes are derived from Arenou et al. (1992)

The signification tests are based on the Kolmogorov-Smirnov criterion for deciding the level at which two samples can be considered to be statistically different. The stars lying in the region $60^0 < l < 90^0$ have been divided into subsamples according to their position in the sky or their parallax, and then these subsamples have been compared. Here we summarize the different tests we have performed and their results.

The pattern of proper motions expected from the galactic rotation does not vary significantly along the longitude interval we are studying, as can be seen in Fig. 2. The distribution functions of proper motions should then be essentially the same for the subsamples consisting respectively of stars lying in the range $72^0 < l < 79^0$, where the anomaly appears, and the rest of stars in $60^0 < l < 90^0$. However, the Kolmogorov-Smirnov criterion shows that both subsamples are different at a significance much below the 1 % level, thus confirming what is suggested by visual inspection of Fig. 2.

A possible cause of the anomaly may be a systematic zonal error in the PPM catalog affecting stars near the galactic equator in $72^0 < l < 79^0$. To explore this possibility, we have extracted from the PPM a sample of 430 A-type stars fainter than magnitude $V = 10$ with longitudes $60^0 < l < 90^0$ and latitudes $| b |< 10^0$. The limitation in magnitude excludes nearby stars whose peculiar velocities would increase the scatter in proper motion, thus smearing out any systematic trends in the mean values. On the other hand, main sequence A stars at the distance of the Cygnus associations are too faint to be included in the PPM catalog, while brighter, evolved A stars should be too old to be physically related to the associations. We have then repeated the Kolmogorov-Smirnov test by comparing the proper motion distribution functions of stars inside the interval $72^0 < l < 79^0$ and outside it, with the result that no statistical difference appears now. Thus, such a zonal error does not seem to exist.

The difference between groups of O and B stars appears again if we consider the distribution function of proper motions with the subsamples divided according to spectrophotometric parallaxes instead of galactic longitudes. The contribution to the proper motion from galactic rotation in this region is almost independent of the parallax for the stars in our sample (see Fig. 3), whose estimated distance is 500 pc or larger. Moreover, the contribution of the cosmic dispersion of velocities to the proper motion for extreme population I stars at these distances should be smaller than the measurement errors. In summary, we would expect the distribution function of proper motions to be only weakly dependent on the distance of our stars. We have thus made two subsamples out of the 167 stars in the interval $72^0 < l < 79^0$, one with distances between 500 pc and 1000 pc and another one with distances greater than 1000 pc. Although the quality of the spectrophotometric parallaxes cannot prevent erroneous classifications of some stars as nearby or distant, the results are conclusive in showing that a difference between both groups does exist, again with a significance level clearly below 1 %. For the stars outside this interval, the difference between both distributions is much smaller and appears only at a significance level of 2 %. Moreover, the mean proper motions of the distant group inside $72^0 < l < 79^0$ are -0"009 yr^{-1} (p.e. 0"003 yr^{-1}, 112 stars), as compared to -0"002 (p.e. 0"005 yr^{-1}, 45 stars) of the nearby group, whereas for the stars outside that interval the mean values are only -0"003 (p.e. 0"005 yr^{-1}, 62 stars), and 0"001 (p.e. 0"005 yr^{-1}, 59 stars) respectively.

We have tried to discard some other possible systematic effects giving rise to the described anomaly. As suggested by Dr. Bastian (private communication), only a strongly magnitude-dependent systematic error might mimic the observed effect. Comparison of the magnitude distribution functions of the subsamples divided according to the galactic longitude of the stars as we did before shows that the difference appears only at a significance level of 13 %, thus being meaningless from the statistical standpoint. Within the interval $72^0 < l < 79^0$, the mean magnitude for the stars in the group with 500 pc $< d <$ 1000 pc differs only in a few hundredths of a magnitude from that of the stars with $d >$ 1000 pc, thus indicating that the distance-dependent effect is not due to systematic magnitude differences.

In conclusion, all our tests on the physical reality of the anomalous proper motions of the O and B stars in $72^0 < l < 79^0$ and $d >$ 1000 pc thus confirm that they arise from the intrinsic motions of the stars, rather than from astrometric systematic errors in the catalogues.

5. New observations

The method of distance determination described by Arenou et al. (1992) is based on a 3-D modelization of the interstellar extinction and its accuracy, yet providing a clear indication of the existence of anomalous proper motions in Cygnus, is rather poor for the purposes of our study (a conservative estimate is a 25% uncertainty in the distance; see discussion in Arenou et al. 1992). In order to have a more reliable and homogeneous set of distances and extinctions towards the stars in the area of Cygnus OB1-OB9, we obtained Strömgren $uvby\beta$ aperture photometry for a selection of them. The selected stars fulfill the following requirements:

- They have catalogued proper motions.
- They have preliminary distances (Arenou et al. 1992) larger than 500 pc.
- They are included in the Hipparcos observing program (Turon et al. 1992).
- They have positions in the range $70^0 < l < 80^0$, $| b |< 10^0$.
- They are not catalogued either as multiple or as variable in the Proposal 99.

Observations were carried out of 48 stars, nearly all those fulfilling these requirements, along four nights with good observing conditions during the period August 1-6, 1991 with the 1.0 m Jacobus Kapteyn Telescope at the Observatorio del Roque de los Muchachos (La Palma, Canary Islands). The instrument used was the two-channel People's photometer available at the facility. Standard stars in the Cygnus region were selected from the database of Strömgren photometry compiled by Hauck & Mermilliod (1990). Four of these standard stars also fulfill the criteria given above, and we used their published photometric values. The list of program stars, with data from the Proposal 99, is given as Table 3a. Table 3b lists the four stars with previously existing *uvbyβ* photometry.

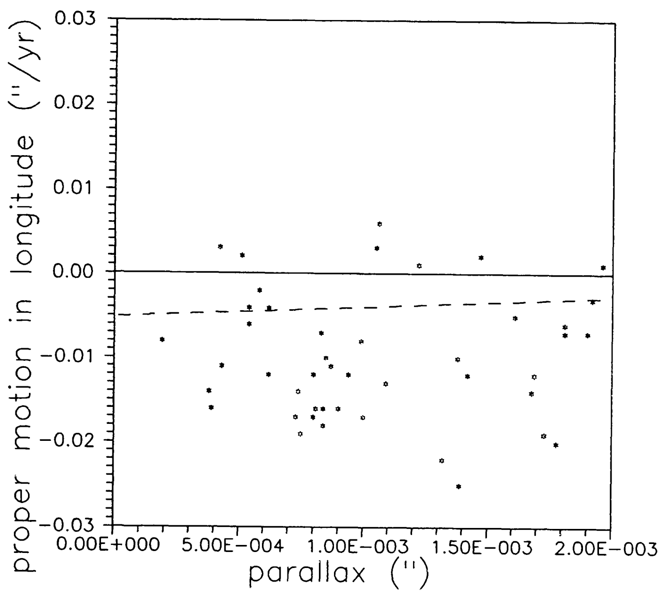

Fig. 4. Derived parallax vs. proper motion of the observed stars plus the ones having already published *uvbyβ* photometry. The dashed line represents the systematic proper motion expected for stars at $l = 75^0$

The observations of our program stars were reduced by the standard procedure described by Crawford & Mander (1966) and Crawford & Barnes (1970). The reduced observations are presented in Table 4.

Table 5 gives the intrinsic colors, excess and parallax for each star. These values have been obtained according to the procedure developed by Figueras et al. (1991) for the "early group" (Strömgren 1966) which makes use of the best calibrations available in the literature. The procedure has been enlarged to take into account evolved stars. For the early-type supergiants we computed the intrinsic colors from the fitting of a polynomial function to the adopted intrinsic color lines of Kilkenny & Whittet (1985) who revised the calibrations given by Shobbrook (1976) and Zhang (1983).

The new parallaxes calculated from Strömgren photometry vs. proper motions in longitude for the 52 stars of our sample are plotted in Fig. 4. Although the number of stars is only 19% that of Fig. 3 and no selection criteria have been introduced regarding peculiarities in proper motions, the deviation from the systematic pattern is still evident. Figure 5 marks the location in a H-R diagram of the clump of stars between 1000 pc and 1600 pc, which clearly appears in Fig. 4, while Fig. 6 highlights the stars having a residual tangential motion in longitude below

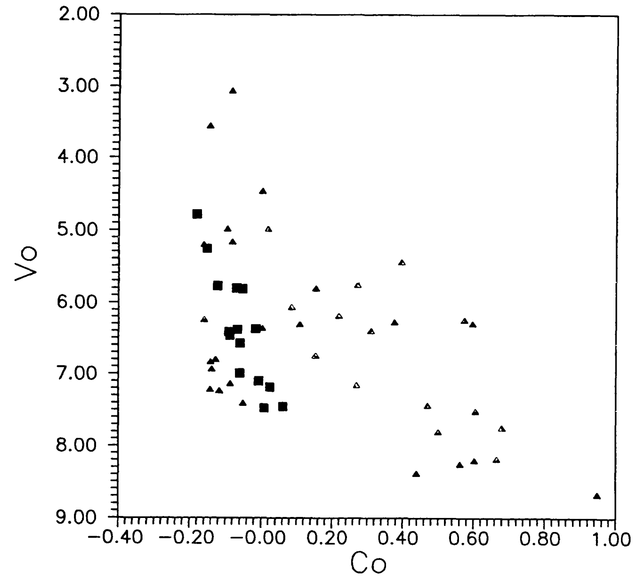

Fig. 5. H-R diagram of the observed stars plus the ones having already published *uvbyβ* photometry. c_0 is a sensitive spectral type indicator in this range (Figueras et al. 1991). Stars lying between 1000 pc and 1600 pc are represented by squares, the rest by triangles

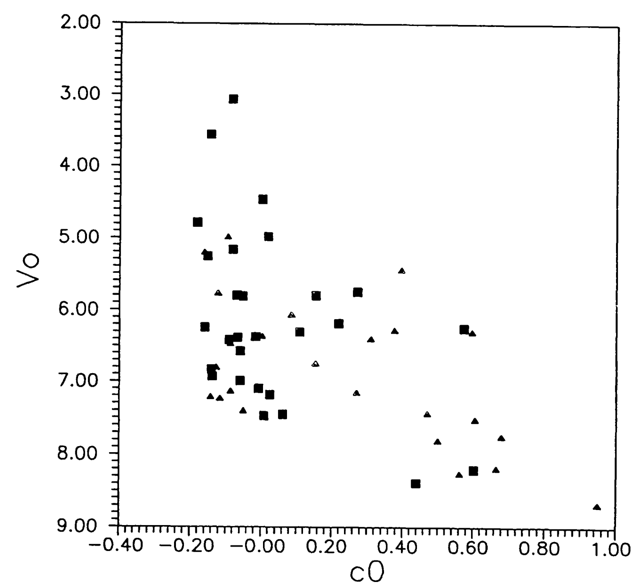

Fig. 6. H-R diagram of the observed stars plus the ones having already published *uvbyβ* photometry. Stars with residual tangential velocities $v < -20$ km s^{-1} are represented by squares, the rest by triangles

-20 km s^{-1} as calculated from the published proper motions, their distances from *uvbyβ* photometry and the

Table 3a. Observed stars

SAO no.	$\alpha(2000)$	$\delta(2000)$	l	b	$\mu_l \cos b$	μ_b	Sp. type	cluster
48681	19 39 07.519	+40 37 37.31	74.17	9.05	0.002	0.013	B0III	
48943	19 53 38.483	+41 21 21.38	76.16	7.02	-0.005	0.001	B2IV	
49173	20 05 38.552	+41 16 47.48	77.27	5.05	-0.012	0.007	B9Iab	
49280	20 10 58.306	+41 21 10.28	77.87	4.25	-0.002	-0.000	O8	
49284	20 11 01.751	+42 07 35.97	78.53	4.66	-0.007	-0.009	O9.5IV	
49290	20 11 16.938	+41 57 32.90	78.41	4.53	-0.004	-0.003	B0IV	
49346	20 14 26.105	+40 19 45.71	77.37	3.14	0.003	-0.004	B0Ia	
49374	20 15 23.517	+42 24 03.35	79.20	4.13	-0.008	-0.002	B5Ia	
49399	20 16 13.806	+40 57 47.74	78.09	3.21	-0.016	-0.006	B1Vn	
49525	20 22 05.409	+40 59 08.09	78.73	2.30	-0.018	0.003	B0.5III	
49545	20 22 44.762	+40 42 52.43	78.58	2.05	-0.017	-0.004	B2III	NGC 6910
49559	20 23 10.735	+40 52 29.90	78.76	2.07	-0.017	0.005	O5	NGC 6910
49563	20 23 18.097	+40 45 32.19	78.68	1.99	-0.025	0.003	B1.5Ia	NGC 6910
49609	20 25 55.046	+41 20 11.49	79.43	1.92	-0.012	0.004	B3II	
49618	20 26 21.526	+41 22 45.68	79.52	1.87	-0.012	0.006	B0.5Ia	
69399	20 05 56.182	+35 40 18.73	72.55	2.01	-0.019	-0.011	B1Ib	NGC 6871
69409	20 06 00.678	+40 03 53.83	76.28	4.34	-0.011	0.002	B0IVp	
69434	20 06 57.647	+36 23 47.11	73.27	2.22	-0.017	-0.015	B0.5III	
69469	20 07 55.509	+35 06 17.34	72.29	1.36	-0.006	-0.006	B6III	
69477	20 08 07.809	+39 45 03.16	76.23	3.83	-0.004	-0.004	B0.5V:	
69491	20 08 36.052	+36 40 18.65	73.68	2.09	-0.016	-0.019	B0.5III	
69498	20 08 45.790	+37 14 13.17	74.18	2.37	-0.014	-0.007	B0IV	
69509	20 09 11.782	+33 55 11.76	71.44	0.50	-0.003	-0.005	B9II	
69520	20 09 28.634	+35 44 00.83	72.99	1.43	-0.014	-0.007	O8	
69539	20 10 11.713	+36 11 28.42	73.45	1.56	-0.006	-0.013	B8V	
69555	20 10 38.236	+33 51 20.77	71.55	0.21	0.002	-0.005	B3V	
69557	20 10 36.686	+37 27 30.09	74.56	2.18	-0.016	-0.008	B1V	
69561	20 10 43.550	+37 27 54.70	74.58	2.17	-0.014	-0.008	B8IV	
69564	20 10 57.039	+35 57 11.41	73.34	1.30	-0.011	-0.006	B1III	NGC 6883
69604	20 12 39.848	+33 29 44.16	71.48	-0.34	0.001	-0.010	B8III	
69654	20 14 09.330	+33 41 10.94	71.81	-0.49	0.008	-0.006	B9IV	
69659	20 14 16.136	+31 59 52.15	70.41	-1.45	0.002	-0.005	B2III	
69672	20 14 25.246	+35 37 20.53	73.45	0.53	0.003	-0.004	B9V	
69676	20 14 30.472	+37 21 13.57	74.90	1.48	-0.006	-0.009	O8e	
69754	20 16 58.868	+37 40 53.19	75.45	1.25	-0.012	0.000	B0.5II	IC 4996
69763	20 17 22.725	+38 14 07.53	75.95	1.50	-0.022	-0.003	B1.5Ib	
69826	20 19 08.506	+39 16 24.26	77.00	1.80	-0.010	-0.003	O7e	
69844	20 19 49.150	+38 20 33.15	76.31	1.16	-0.022	-0.004	B3III	
69880	20 21 07.491	+39 01 53.62	77.02	1.34	-0.020	0.003	B2III	
69920	20 22 35.561	+38 07 45.16	76.44	0.59	-0.019	-0.003	B1Iab	
69942	20 23 26.315	+38 56 20.84	77.20	0.92	-0.013	-0.004	B0Ib	
69995	20 24 58.762	+39 50 21.36	78.11	1.20	-0.010	-0.003	B8III	
70181	20 33 05.088	+31 39 25.80	72.43	-4.92	-0.012	0.004	B1.5V	
70194	20 33 30.372	+32 54 27.83	73.49	-4.25	-0.007	-0.001	B2V	
70255	20 36 18.227	+37 25 02.51	77.45	-2.02	-0.008	-0.015	O9V	
70410	20 42 41.092	+36 22 50.44	77.41	-3.66	-0.012	-0.011	B0.5Ib	
70442	20 44 26.598	+31 41 45.15	73.92	-6.83	0.006	-0.001	B 1 III(N)	
70590	20 51 30.965	+37 59 22.11	79.77	-4.03	-0.006	-0.007	B2V	
70953	21 07 55.428	+33 23 49.58	78.44	-9.54	0.003	-0.007	O9p	

Table 3b. Stars with photometry from Hauck & Mermilliod (1990)

SAO no.	$\alpha(2000)$	$\delta(2000)$	l	b	$\mu_l \cos b$	μ_b	Sp. type	cluster
49080	20 00 59.948	+42 00 30.33	77.43	6.17	-0.016	0.008	B0III	
69457	20 07 41.448	+34 25 22.72	71.69	1.03	0.001	-0.002	B5Ib	
69725	20 16 28.190	+37 03 22.78	74.87	0.99	-0.007	-0.009	B6III	
70596	20 52 00.424	+32 50 56.43	75.83	-7.36	0.002	-0.006	B3III	

standard values for the galactic rotation and the solar motion.

It is interesting to compare the distance of Cygnus OB1-OB9 to that of Cygnus OB2. Torres-Dodgen et al. (1991) used the calibration of Humphreys & McElroy (1984) to obtain absolute magnitudes. We cannot apply our procedure to their observed stars, because of the lack of $H\beta$ values, which are necessary in the Balona & Shobbrook (1984) calibration. Nevertheless, when the calibration of Humphreys & McElroy is applied to our stars according to their spectral types, a mean difference in absolute magnitude of -0.7 (p.e. 0.5) is found, in the sense (HM - BS). Applying the same difference to their observed stars, the distance modulus derived for Cygnus OB2 should be 10.5 mag with the Balona & Shobbrook calibration. Thus, the association may be placed at a distance of 1250 pc, similar to that found for the bulk of stars belonging to Cygnus OB1-OB9.

6. Discussion

Taking 1200 pc as the mean distance of the group of stars with anomalous proper motions, the observed difference of about 0"006 - 0"008 yr^{-1} with respect to the circular rotation implies a velocity perpendicular to the line of sight of nearly 40 km s^{-1}. We have detected no such systematic deviations neither on the proper motions in latitude nor in radial velocity. Nevertheless, due to the large distance of these stars, a group velocity of just 20 km s^{-1} would no longer be detectable from our sample. The same can be said about radial velocities, which are available only for a reduced number of stars. Thus, there exists an uncertainty about the spatial orientation of the anomalous motions, the perpendicularity to the visual line being only a rough estimate. We should point out that systematic deviations from the circular motions resulting in a stream towards the galactic center are to be expected whithin spiral arms inside the galactic corrotation circle, as predicted by the spiral density wave theory (Lin et al. 1969; Rohlfs 1977). Nevertheless, the amplitude of the velocity perturbation should have a significantly lower value. Lin et al. (1969) and Strauss & Pöppel (1976) found wavelike deviations of up to 10 km s^{-1} in the kinematics of the HI in our Galaxy; and Comerón & Torra (1991) obtained 5.6 ± 1.7 km s^{-1} for the amplitude from an extended sample of O and B stars. Thus, it seems clear that the contribution of the spiral arm kinematics cannot account for the entire amount of the anomalous motions.

Based on this spatial and kinematic arrangement of Cygnus OB2, the Superbubble around it and Cygnus OB1-OB9 near the edge of the Superbubble and moving away from Cygnus OB2, we propose an alternative explanation of the observed facts. It has been shown by analytical as well as numerical simulations that the mechanical energy injected into a small volume of the ISM by stellar winds and supernova explosions occurring in young OB associations cause large bubble-shaped disturbances to grow in the ISM (Chevalier 1977; Bruhweiler et al. 1980; Mac Low & McCray 1988). Early in the life of the bubble, a cold, dense shell forms where the material encountered by the expanding bubble is accreted. Eventually, the surface density of the shell may surpass the threshold for gravitational instability, and dense, bound structures may detach from the shell further evolving into new star forming regions (Olano 1982). According to this picture, stellar and supernova activity in Cygnus OB2 initiated the sweeping of the surrounding ISM more than 10^7 years ago forming a rapidly expanding hot cavity which is now observed as the Cygnus Superbubble. The high densities of the local ISM allowed to form a massive shell which finally disrupted under its own gravity. Some of the shell fragments are observed today as Cygnus OB1, OB9 and other possible stellar groups in that region. As parts of the gravitationally bound groups started to collapse, the drag force of the rest ISM over them was progressively reduced; thus, their current velocities are a remnant of the expanding motion of the shell in the epoch of their formation. A more detailed study of this scenario and a quantitative derivation of the most relevant involved parameters as deduced from the available observations will be presented in a further paper (Comerón & Torra, in preparation).

Acknowledgements. We are pleased to thank J. Martí for participating in the observations, Dr. P.J. Andrews for technical support at the Jacobus Kapteyn Telescope and Dr. M.O. Mennessier for permitting us to use Proposal 99 data. Valuable advices given to us by Dr. U. Bastian on the possible systematic effects in the PPM are gratefully acknowledged. Helpful comments by Dr. M. Crézé leading to improvement of this paper are appreciated. This research has been financially supported by the CICYT under contract ESP88-0731 and Acciones Integradas Hispano-Francesas. The observing run on La Palma was supported by the DGICYT.

References

Arenou F., Grenon M., Gómez A.E. 1992, A&A 258, 104
Balona L.A., Shobbrook R.R. 1984, MNRAS 211, 375
Blitz L., Fich M., Stark A.A. 1982, ApJS 49, 183
Bochkarev N.G., Sitnik T.G. 1985, Ap. Space Sci. 108, 237
Bruhweiler F.C., Gull T.R., Kafatos M., Sofia S. 1980, ApJ 238, L27
Cash W., Charles P., Bowyer S., Walter F., Garmire G., Riegler G., 1980, ApJ 238, L71
Chevalier R.A. 1977, ARA&A 15, 175
Comerón F., Torra J. 1991, A&A 241, 57
Crawford D.L., Barnes J.V. 1970, AJ 75, 978
Crawford D.L., Mander J. 1966, AJ 71, 114

Table 4. *uvbyβ* photometry of the observed stars

SAO no.	V	$(b-y)$	m_1	c_1	$H\beta$	no. obs.
48681	7.733 ± 0.036	0.019 ± 0.005	0.016 ± 0.006	−0.059 ± 0.007	2.590 ± 0.009	4
48943	6.971 ± 0.036	−0.046 ± 0.005	0.063 ± 0.006	0.163 ± 0.007	2.642 ± 0.009	4
49173	7.446 ± 0.058	0.332 ± 0.006	−0.013 ± 0.007	0.626 ± 0.007	2.600 ± 0.009	4
49280	8.037 ± 0.028	0.167 ± 0.005	−0.019 ± 0.007	−0.071 ± 0.007	2.598 ± 0.007	6
49284	8.254 ± 0.029	0.304 ± 0.007	−0.066 ± 0.007	−0.006 ± 0.007	2.604 ± 0.008	6
49290	8.751 ± 0.029	0.235 ± 0.006	−0.045 ± 0.008	−0.047 ± 0.008	2.606 ± 0.008	6
49346	7.517 ± 0.035	0.536 ± 0.006	−0.124 ± 0.012	0.017 ± 0.008	2.574 ± 0.009	4
49374	8.723 ± 0.065	0.680 ± 0.018	−0.132 ± 0.024	0.284 ± 0.007	2.547 ± 0.023	6
49399	7.852 ± 0.029	0.061 ± 0.004	0.017 ± 0.008	0.027 ± 0.008	2.614 ± 0.007	6
49525	8.229 ± 0.033	0.174 ± 0.005	−0.030 ± 0.007	−0.004 ± 0.007	2.621 ± 0.008	6
49545	8.099 ± 0.029	0.105 ± 0.004	0.016 ± 0.007	0.067 ± 0.007	2.629 ± 0.007	6
49559	8.493 ± 0.036	0.742 ± 0.005	−0.169 ± 0.012	−0.017 ± 0.008	2.573 ± 0.010	4
49563	6.823 ± 0.098	0.827 ± 0.008	−0.221 ± 0.010	0.083 ± 0.012	2.550 ± 0.009	4
49609	7.710 ± 0.044	0.242 ± 0.006	−0.028 ± 0.009	0.170 ± 0.009	2.616 ± 0.009	4
49618	7.303 ± 0.097	0.778 ± 0.008	−0.163 ± 0.009	0.021 ± 0.013	2.574 ± 0.010	4
69399	7.217 ± 0.043	0.231 ± 0.007	−0.036 ± 0.006	−0.010 ± 0.007	2.575 ± 0.009	4
69409	8.137 ± 0.037	0.181 ± 0.004	−0.034 ± 0.006	−0.082 ± 0.006	2.581 ± 0.007	6
69434	7.903 ± 0.038	0.231 ± 0.005	−0.041 ± 0.006	−0.024 ± 0.006	2.592 ± 0.007	6
69469	8.090 ± 0.031	0.002 ± 0.004	0.082 ± 0.006	0.513 ± 0.006	2.719 ± 0.007	6
69477	8.405 ± 0.035	0.119 ± 0.004	0.007 ± 0.006	−0.005 ± 0.006	2.608 ± 0.008	6
69491	7.368 ± 0.041	0.113 ± 0.005	0.006 ± 0.007	−0.022 ± 0.007	2.594 ± 0.009	4
69498	8.559 ± 0.044	0.145 ± 0.005	0.003 ± 0.007	0.057 ± 0.007	2.615 ± 0.008	6
69509	7.888 ± 0.035	0.046 ± 0.004	0.069 ± 0.006	0.622 ± 0.006	2.703 ± 0.007	6
69520	7.723 ± 0.041	0.239 ± 0.006	−0.007 ± 0.006	−0.094 ± 0.006	2.563 ± 0.007	6
69539	8.605 ± 0.054	0.023 ± 0.006	0.092 ± 0.008	0.577 ± 0.010	2.735 ± 0.013	2
69555	7.695 ± 0.037	−0.006 ± 0.007	0.085 ± 0.008	0.482 ± 0.009	2.700 ± 0.009	4
69557	8.445 ± 0.029	0.126 ± 0.005	0.014 ± 0.007	0.106 ± 0.008	2.625 ± 0.008	6
69561	8.941 ± 0.029	0.129 ± 0.006	0.057 ± 0.007	0.635 ± 0.008	2.723 ± 0.007	6
69564	7.779 ± 0.029	0.166 ± 0.006	−0.007 ± 0.007	−0.004 ± 0.007	2.606 ± 0.007	6
69604	8.025 ± 0.029	0.025 ± 0.004	0.079 ± 0.006	0.693 ± 0.007	2.721 ± 0.008	6
69654	8.575 ± 0.030	0.050 ± 0.004	0.095 ± 0.006	0.683 ± 0.007	2.765 ± 0.007	6
69659	7.249 ± 0.035	0.176 ± 0.006	−0.020 ± 0.007	0.139 ± 0.009	2.610 ± 0.010	4
69672	8.695 ± 0.030	−0.021 ± 0.005	0.158 ± 0.007	0.949 ± 0.008	2.859 ± 0.008	6
69676	7.100 ± 0.035	0.321 ± 0.006	−0.045 ± 0.010	−0.075 ± 0.008	2.557 ± 0.009	4
69754	7.612 ± 0.034	0.313 ± 0.005	−0.058 ± 0.010	0.028 ± 0.008	2.584 ± 0.009	4
69763	6.877 ± 0.045	0.384 ± 0.006	−0.058 ± 0.006	0.102 ± 0.008	2.577 ± 0.008	6
69826	7.292 ± 0.062	0.373 ± 0.006	−0.024 ± 0.008	−0.062 ± 0.010	2.582 ± 0.009	4
69844	7.330 ± 0.034	0.287 ± 0.006	−0.017 ± 0.007	0.344 ± 0.008	2.634 ± 0.008	6
69880	7.724 ± 0.041	0.272 ± 0.008	−0.023 ± 0.013	0.288 ± 0.017	2.626 ± 0.014	2
69920	8.311 ± 0.073	0.857 ± 0.006	−0.199 ± 0.007	0.173 ± 0.010	2.579 ± 0.008	6
69942	8.246 ± 0.055	0.638 ± 0.006	−0.156 ± 0.008	0.056 ± 0.007	2.579 ± 0.008	6
69995	8.670 ± 0.028	−0.005 ± 0.005	0.094 ± 0.007	0.452 ± 0.006	2.704 ± 0.007	6
70181	7.759 ± 0.030	0.107 ± 0.005	−0.010 ± 0.007	0.046 ± 0.008	2.492 ± 0.008	6
70194	7.322 ± 0.032	−0.050 ± 0.006	0.078 ± 0.008	0.278 ± 0.009	2.670 ± 0.009	4
70255	8.764 ± 0.055	0.584 ± 0.005	−0.199 ± 0.008	0.013 ± 0.007	2.601 ± 0.008	6
70410	8.037 ± 0.040	0.342 ± 0.005	−0.095 ± 0.008	0.058 ± 0.007	2.586 ± 0.008	6
70442	7.839 ± 0.041	0.237 ± 0.004	−0.081 ± 0.006	0.069 ± 0.006	2.603 ± 0.007	6
70590	7.217 ± 0.042	0.110 ± 0.007	0.025 ± 0.007	0.347 ± 0.007	2.654 ± 0.009	4
70953	7.744 ± 0.036	−0.004 ± 0.008	0.011 ± 0.009	−0.118 ± 0.007	2.593 ± 0.009	4

Table 5. Deduced parameters of the observed stars

SAO no.	$(b-y)_0$	m_0	c_0	δm_0	$E(b-y)$	M_V	π"	$M_V - M_{V_{ZAMS}}$	remarks
48681	-0.124	0.063	-0.086	0.002	0.143	-4.33	0.00051	0.60	
48943	-0.101	0.081	0.153	0.005	0.055	-2.24	0.00161	0.62	
49080	-0.129	0.087	-0.138	-0.026	0.212	-5.13	0.00039	0.67	photometry from H&M
49173	0.050	0.080	0.572	0.030	0.282	-4.79	0.00062	4.78	
49280	-0.128	0.078	-0.127	-0.017	0.295	-4.41	0.00058	0.13	
49284	-0.124	0.075	-0.087	-0.010	0.428	-3.97	0.00083	0.22	
49290	-0.127	0.075	-0.116	-0.012	0.362	-4.13	0.00054	0.00	
49346	-0.076	0.078	-0.099	-0.014	0.612	-4.94	0.00107	1.04	
49374	-0.019	0.099	0.151	-0.012	0.699	-7.73	0.00020	6.10	
49399	-0.117	0.076	-0.007	-0.003	0.178	-3.29	0.00084	0.46	
49525	-0.122	0.068	-0.060	0.000	0.296	-3.42	0.00084	0.01	
49545	-0.114	0.088	0.025	-0.013	0.219	-2.84	0.00100	0.30	
49559	-0.110	0.115	-0.181	-0.058	0.861	-5.69	0.00079	0.54	
49563	-0.071	0.075	-0.088	-0.010	0.898	-6.21	0.00145	2.47	
49609	-0.024	0.060	0.120	0.024	0.266	-2.91	0.00127	1.09	
49618	-0.098	0.126	-0.145	-0.066	0.876	-5.30	0.00169	0.73	
69399	-0.064	0.061	-0.066	0.006	0.295	-4.73	0.00080	1.25	
69409	-0.130	0.069	-0.141	-0.008	0.311	-5.02	0.00043	0.52	
69434	-0.125	0.076	-0.092	-0.012	0.356	-4.31	0.00073	0.51	
69457	0.019	0.055	0.398	0.047	0.144	-4.13	0.00118	3.56	photometry from H&M
69469	-0.068	0.105	0.500	0.002	0.070	-0.69	0.00201	0.45	
69477	-0.121	0.086	-0.051	-0.018	0.240	-3.65	0.00062	0.35	
69491	-0.122	0.084	-0.067	-0.017	0.235	-4.10	0.00081	0.61	
69498	-0.115	0.089	0.008	-0.015	0.260	-3.21	0.00074	0.51	
69509	0.046	0.069	0.622	0.044	0.000	-1.09	0.00160	1.24	
69520	-0.106	0.107	-0.159	-0.048	0.345	-5.87	0.00038	1.08	
69539	-0.062	0.120	0.561	-0.010	0.085	-0.46	0.00181	0.42	
69555	-0.070	0.106	0.470	-0.001	0.064	-1.00	0.00207	0.66	
69557	-0.110	0.092	0.061	-0.014	0.236	-2.80	0.00090	0.56	
69561	-0.047	0.115	0.602	-0.003	0.176	-0.68	0.00168	0.77	
69564	-0.122	0.088	-0.059	-0.020	0.288	-3.74	0.00087	0.35	
69604	-0.044	0.102	0.680	0.014	0.069	-0.80	0.00196	1.15	
69654	-0.044	0.126	0.665	-0.011	0.094	-0.08	0.00224	0.37	
69659	-0.108	0.074	0.085	0.007	0.284	-3.13	0.00147	1.07	
69672	-0.027	0.160	0.948	-0.025	0.006	0.89	0.00278	0.36	
69676	-0.132	0.104	-0.161	-0.046	0.453	-6.17	0.00054	1.36	
69725	-0.058	0.093	0.596	0.019	0.043	-2.31	0.00190	2.38	photometry from H&M
69754	-0.056	0.064	-0.042	0.006	0.369	-4.29	0.00086	1.08	
69763	-0.040	0.082	0.021	-0.007	0.424	-4.42	0.00127	1.85	
69826	-0.102	0.133	-0.152	-0.073	0.475	-5.09	0.00085	0.42	
69844	-0.090	0.107	0.272	-0.012	0.377	-2.38	0.00240	1.34	
69880	-0.095	0.098	0.218	-0.005	0.367	-2.59	0.00178	1.31	
69920	-0.117	0.122	-0.012	-0.051	0.974	-4.38	0.00196	1.49	
69942	-0.068	0.077	-0.078	-0.011	0.706	-4.63	0.00106	1.01	
69995	-0.073	0.117	0.439	-0.013	0.068	-0.92	0.00138	0.48	
70181	-0.116	0.063	0.004	0.010	0.223	-0.92	0.00120	-1.81	
70194	-0.090	0.091	0.270	0.004	0.040	-1.56	0.00181	0.51	
70255	-0.128	0.036	-0.122	0.026	0.712	-4.30	0.00099	0.08	
70410	-0.049	0.034	-0.016	0.038	0.391	-4.12	0.00080	1.19	
70442	-0.116	0.035	0.002	0.038	0.353	-3.53	0.00106	0.78	
70590	-0.086	0.090	0.310	0.008	0.196	-1.88	0.00222	1.00	
70596	-0.080	0.089	0.376	0.012	0.036	-1.41	0.00292	0.76	photometry from H&M
70953	-0.130	0.053	-0.142	0.008	0.126	-4.67	0.00042	0.16	

Dickel H.R., Wendker H.J. 1978, A&A 66, 289
Elmegreen D.M. 1985, in "The Milky Way Galaxy", eds. H. van Woerden et al., IAU Symp. 106, D. Reidel Publ. Co.
Figueras F., Torra J., Jordi C. 1991, A&AS 87, 319
Fricke W., Schwan H., Lederle T. 1988, "Fifth Fundamental Catalogue (FK5)", Veröff. Astronomisches Rechen-Institut 32
Garmany C.D., Vacca W.D. 1991, PASP 103, 347
Garmany C.D., Stencel R.E. 1992, A&AS 94, 211
Gómez A.E., Crifo F., Turon C. 1989a, in "The Hipparcos Mission", vol. II, eds. M.A.C. Perryman & C. Turon, ESA SP-1111
Gómez A.E., Morin D., Arenou F. 1989b, in "The Hipparcos Mission", vol. II, eds. M.A.C. Perryman & C. Turon, ESA SP-1111
Hauck B., Mermilliod J.C. 1990, A&AS 86, 107
Heiles C. 1979, ApJ 229, 533
Heiles C. 1984, ApJS 55, 585
Humphreys R.M. 1978, ApJS 38, 309
Humphreys R.M., McElroy D.B. 1984, ApJ 284, 565
Hutchings J.B. 1981, PASP 93, 50
Jahreiβ, H. 1989, in "The Hipparcos Mission", vol. II, eds. M.A.C. Perryman & C. Turon, ESA SP-1111
Janes K.A., Tilley C., Lyngå G. 1988, AJ 95, 771
Jaschek M. 1978, Bull. Inf. CDS 15, 121
Kerr F.J., Lynden-Bell D. 1986, MNRAS 221, 1023
Kilkenny D., Whittet D.C.B. 1985, MNRAS 216, 127
Leitherer C., Hefele H., Stahl O., Wolf B. 1982, A&A 108, 102
Lin C.C., Yuan C., Shu F.H. 1969, ApJ 155, 721
Lockman F.J. 1989, ApJS 71, 469
Lozinskaya T.A., Sitnik T.G. 1988, Sov. Astron. Lett. 14, 100
Lozinskaya T.A., Repin S.V. 1990, Sov. Astron. 34, 580
Lucke P.B. 1978, A&A 64, 381
LyngåG. 1987, "Catalogue of Open Cluster Data (5th edition)", CDS Cat. no. VII-92
Mac Low M.-M., McCray R. 1988, ApJ 324, 776
Mennessier M.O., Gómez A.E. 1989, in "The Hipparcos Mission", vol. II, eds. M.A.C. Perryman & C. Turon, ESA SP-1111 (Appendix C)
Olano C.A. 1982, A&A 112, 195
Piepenbrink A., Wendker H.J. 1988, A&A 191, 313
Röser S., Bastian U. 1991, "PPM Star Catalogue", Spektrum Acad. Publ.
Rohlfs K. 1977, "Lectures in Density Wave Theory", Springer- Verlag
Ruprecht J. 1966, Trans. IAU, vol. XIIB, 336
Strauss F.M., Pöppel, W. 1976, ApJ 204, 94
Strömgren B. 1966, ARA&A 4, 433
St. Louis N., Smith L.J. 1991, A&A 252, 781
Shobbrook R.R. 1976, MNRAS 176, 673
Torres- Dodgen A.V. 1990, PASP 102, 1406
Torres- Dodgen A.V., Tapia M., Carroll M. 1991, MNRAS 249, 1
Turon C. et al. 1992, "The Hipparcos Input Catalogue", ESA SP-1136
Wendker K.J. 1984, A&AS 58, 291
Zhang E.H. 1983, AJ 88, 825